Korean J. Chem. Eng., 33(8), 2502-2512 (2016)
DOI: 10.1007/s11814-016-0072-z

pISSN: 0256-1115
eISSN: 1975-7220

Optimization of the preparation of activated carbon from palm kernel shell for methane adsorption using Taguchi orthogonal array design

Syed Shatir Asghrar Syed-Hassan† and Mohd Saufi Md Zaini

Faculty of Chemical Engineering, Universiti Teknologi MARA, 40450 Shah Alam, Selangor, Malaysia
(*Received 1 December 2015 • accepted 4 March 2016*)

Abstract−The preparation of activated carbon from palm kernel shell for methane adsorption was studied. Taguchi orthogonal array design was employed to optimize the preparation of activated carbon. The statistical results show that the optimized conditions are the impregnation ratio of 0.55, the activation temperature of 900 °C and the activation time of 150 min. The impregnation ratio has the most influence on methane adsorption based on S/N ratio analysis. The mathematical model was developed using regression analysis as a function of independent variables. The results of experiment using optimum conditions fall within the predicted value obtained from the developed model. Activated carbon prepared at optimum conditions which have the highest BET surface area of 1,548.0 m^2/g and the total pore volume of 1.0 cm^3/g recorded the highest methane uptake compared to other conditions. The equilibrium data of the adsorption characteristic fitted favourably to the Freundlich isotherm.

Keywords: Taguchi Orthogonal Array Design, Activated Carbon, Methane Adsorption, Adsorption Isotherm, Palm Kernel Shell

INTRODUCTION

Natural gas is a promising alternative to conventional fuels due to its huge resources, sustainable energy, low price and various environmental advantages. Natural gas burns cleaner than gasoline, emitting fewer hydrocarbon and 90% less carbon monoxide [1]. To be used as a transportation fuel, natural gas has to be stored in a special storage system owing to its low volumetric energy density. Current method of storing natural gas for the on-board application is via the compressed natural gas technology (CNG). This technology, however, is not viable due to the high storage pressure (up to 250 bar) which requires heavy storage and high compression cost [2]. An alternative method of storing natural gas at relatively low pressure (35-40 bar) is through adsorption in porous materials, which is also referred to as adsorbed natural gas technology (ANG).

The production of suitable adsorbent for ANG, particularly carbon-based adsorbent continues to be an active area of scientific research. Among the numerous adsorbents available, activated carbon is recognized as a good adsorbent due to its unique adsorptive properties such as high degree of surface reactivity, large microporous volume and extremely high surface area (up to 2,500 m^2/g) [3]. In recent years, extensive researches have been carried out to utilize agro-industrial lignocellulosic wastes that are abundantly available and inexpensive for the production of activated carbon. Previous works show that agricultural biomasses have high carbon content and low ash content, which is appropriate for activated carbon precursors [4]. One of these low-cost biomasses is palm kernel shell (PKS), which can be found widely in Malaysia. PKS is regarded as a good candidate of producing high quality activated carbon since it has high density, low ash content and high percentage of carbon [5].

Production of the most suitable activated carbon for the gas adsorption application requires consideration of various factors such as chemical agent, impregnation ratio, activation temperature, and activation time. Thus, it is essential to do varieties of experimental works. To reduce the number of experiments efficiently, a statistical design of experiments is usually adopted. Taguchi methodology is a valuable tool, providing a systematic way to optimize design of performance and quality of product through "orthogonal array design". It also organizes parameters and the level affecting the process with respect to all control factors with minimum amount of experimentation [6]. Unlike the conventional methods which use only mean value of response to determine the optimum level without showing the variability of data set, the Taguchi method takes into account both mean value and the variance. An important aspect that needs to be considered is the signal-to-noise (S/N) ratio. S/N ratio is an analytical medium used to determine the best levels which contribute to optimum response value. Fig. 1 describes a brief overview of the Taguchi design of experiment for the optimization of activated carbon preparation reported in this paper.

Taguchi method has been implemented by many researchers and it is applied largely in various optimization processes. This experimental design uses orthogonal arrays to organize the parameters affecting the process and the level at which they should be varied. Instead of having to test all possible combinations like a full factorial design, the Taguchi method tests pairs of combinations. This allows for the collection of the necessary data to determine which factors most affect the product quality with minimum number of experimentation. This ensures minimum use of resources, saves

†To whom correspondence should be addressed.
E-mail: shatir@salam.uitm.edu.my, syedshatir@gmail.com

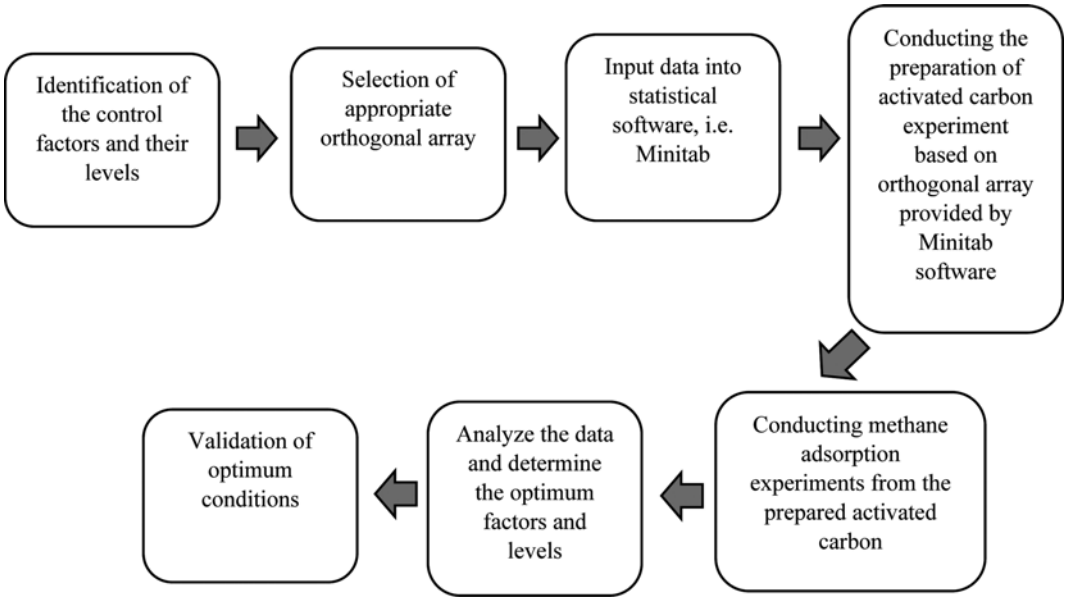

Fig. 1. Overview of Taguchi methodology for methane adsorption in this study.

time and lowers the production cost. Many previous studies on the production of activated carbon also used Taguchi methodology to analyze data for the optimization purposes. For example, Kundu et al. [6] investigated the optimum conditions of preparation of activated carbon for methylene blue adsorption on palm shell. They studied four factors in four levels such as microwave power, time, impregnation ratio and concentration of acid. On the other hand, Hui Deng et al. [7] applied the Taguchi method to optimize the preparation of activated carbon from cotton stalk with phosphoric acid (H_3PO_4). They found that radiation time was a more important factor than concentration of H_3PO_4, radiation power and impregnation time, based on analysis of variance (ANOVA) and S/N ratio analysis. Meanwhile, Mahboub et al. [8] employed the Taguchi method to optimize the production of activated carbon from coconut shell. They investigated the effect of five parameters, which are impregnation ratio, CO_2 flow, carbonization temperature, carbonization time and soaking time to the porosity of activated carbon. The ultimate goal in those researches is to obtain the optimum conditions of methane uptake through wet mesoporous activated carbon. No study to date, however, has reported the application of Taguchi method in the preparation of activated carbon from $ZnCl_2$ treated PKS with sequential combination of CO_2 and steam activation for methane adsorption.

In this study we adopted Taguchi orthogonal array experimental design to obtain optimum conditions for the preparation of activated carbon from PKS for methane adsorption. PKS were treated with $ZnCl_2$ prior to carbonization and activation processes. The activation using sequential combination (as opposed to the usual simultaneous combination) of CO_2 and steam was used in this study. It was documented before that the mixture (simultaneous combination) of steam and CO_2 provides positive effects to the production of activated carbon [28]. The use of sequential combination of CO_2 and steam in this study may provide additional understanding to the different roles of activating agents and their inter-influence during the activation of carbon materials. The effects of preparation variables such as impregnation ratio, activation temperature and activation time on methane adsorption were subsequently investigated. Comparisons of adsorbent's physical characteristics were made between the optimum conditions and other selected conditions.

EXPERIMENTAL

1. Raw Material Preparation

Oil palm kernel shell (PKS) was used as activated carbon precursor in this study. PKS was obtained from Sime Darby Research and Development Centre (R&D) in Carey Island, Malaysia. PKS was washed with distilled water to remove dust and impurities. The washed PKS was sun-dried for 48 hours and further dried in an oven at 110 °C overnight to remove moisture and to preserve from biological degradation. The dried PKS was crushed and sieved to obtain particles sizes in the range of 0.5 to 1.0 mm.

2. Preparation of Activated Carbon

Dried PKS with the mass of 110 (±0.1) g was mixed into 220 mL zinc chloride solution (98+% purity from Acros Organics) at various ratios between 0.1-0.55 (w/w). The mixture was stirred by a magnetic stirrer in a beaker at 80 °C for 3 hours. The mixture was then dried in an oven at 110 °C until the PKS achieved complete dryness. Fig. 2 shows the experimental setup for carbonization and activation processes. The setup consists of a double layer stainless steel reactor. The inner part of the reactor is 50 mm in diameter and 400 mm in length, while the outer part of the reactor is 63 mm in diameter and 500 mm in length. The dried $ZnCl_2$-treated PKS was placed on the perforated plate, which was covered with a fine stainless steel mesh, inside the inner part of the reactor. The biomass was carbonized under nitrogen flow of ~190 cm^3/min until the temperature reached the desired activation temperature. N_2 gas was then switched to CO_2 and followed by steam

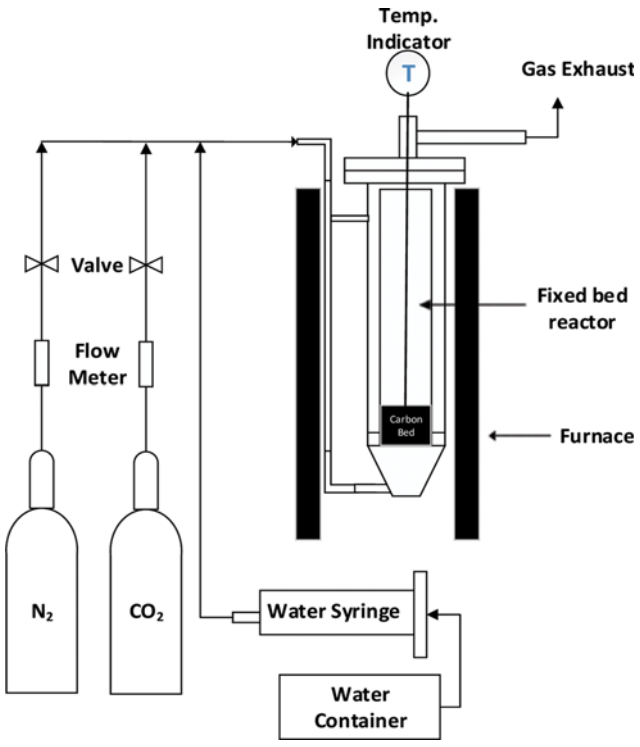

Fig. 2. Schematic diagram of the set-up for the preparation of activated carbon.

sequentially for a certain period of time. The activated carbon obtained was washed under stirring with 0.1 M hydrochloric acid for one hour and further washed six times with hot distilled water (30 minutes each) to remove the remaining chemicals.

3. Methane Adsorption by Volumetric Method

20 (±0.1) g of activated carbon sample was weighed and placed into high pressure stainless steel adsorbent cell and degassed for several hours to remove any impurity at room temperature. A schematic diagram of experimental set-up is shown in Fig. 3. Two pressure transmitters, model TPS20-G27F8-00 (ranged 0-20 kg/cm^3 with accuracy ±0.001) manufactured by Murr Electronic, were used to measure the pressure. Methane gas was injected using needle valve up to 10 (±0.001) bar continuously. The number of moles of methane uptake was determined from the mass balance by the application of ideal gas equation of states.

$$n_{ads}/mass_{AC}=\left[(P_{ref_1}-P_{ref_2})\frac{V_{ref}}{RT}-(P_{ad_2}-P_{ad_1})\frac{V_{ad}}{RT}\right]/mass_{AC} \quad \text{(mol/kg)} \quad (1)$$

In the above equation, $n_{ads}/mass_{AC}$ is the methane uptake (mol/kg), P_{ref} is the pressure at reference cell (bar), V_{ref} is the volume of reference cell (cm^3), T_{ref} is the temperature of reference cell (K), P_{ad} is the pressure of adsorption cell (bar), V_{ad} is the volume of adsorption cell (cm^3), T_{ad} is the temperature of adsorption cell (K), the subscript "1" and "2" represent before and after injection of methane, respectively, and R is the gas constant (cm^3·bar/mol·K).

4. Taguchi Experimental Design

In this research, L_{16} orthogonal array with three control factors and four levels was selected with the aim of obtaining the optimized condition that would give high methane uptake. The parameters and their levels selected are impregnation ratio, activation temperature and activation time (Table 1). The design matrix (summarized in Table 2) of the experiment was provided by the Minitab software 14. In the Taguchi method, the quality of response is measured by the consistencies of its performance. There are three main types of S/N ratio, which are smaller the better, nominal the best and larger the better. Since the aim of this study is to obtain the value of response (methane adsorption) as high as possible, the larger the better of S/N equation is used (Eq. (2)). Note that in the equation

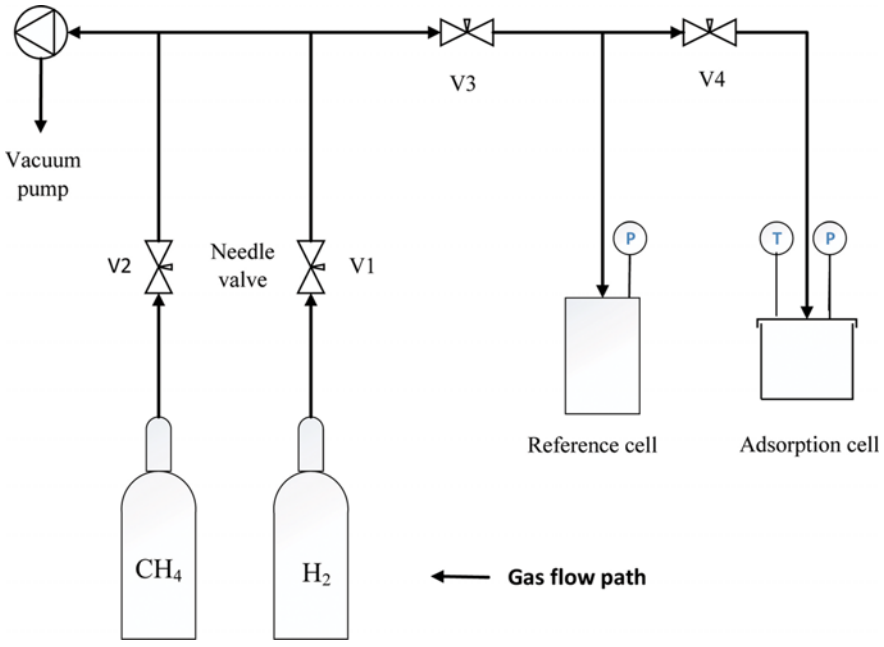

Fig. 3. Schemtic diagram of the methane adsorption unit.

Table 1. Control factors and their levels

Control factors	Level 1	Level 2	Level 3	Level 4
Impregnation ratio	0.1	0.25	0.4	0.55
Activation temperature (°C)	750	800	850	900
Activation time (min)	60	90	120	150

Table 2. Design matrix of experiments and results (response)

No	Control factors		
	Impregnation ratio	Activation temp.	Activation time
1	0.1	750	60
2	0.1	800	90
3	0.1	850	120
4	0.1	900	150
5	0.25	750	90
6	0.25	800	60
7	0.25	850	150
8	0.25	900	120
9	0.4	750	120
10	0.4	800	150
11	0.4	850	60
12	0.4	900	90
13	0.55	750	150
14	0.55	800	120
15	0.55	850	90
16	0.55	900	60

is equal to the deviation of each response (methane adsorption).

$$\frac{S}{N} = -10\log\left(\frac{1}{N_i}\Sigma_{U=1}^{N_i}\frac{1}{Y_u^2}\right) \quad (2)$$

N_i in the equation is the number of experimental replication, while $\left(\frac{1}{N_i}\Sigma_{U=1}^{N_i}\frac{1}{Y_u^2}\right)$ is the mean of sum squares of reciprocal of measured data.

5. Characterisation of Activated Carbons

The produced activated carbons at optimum and selected conditions were characterized by nitrogen adsorption/desorption at 77 K using a Quantachrome Autosorb Automated Gas Adsorption system. Prior to the analysis, each sample was degassed at 300 °C for 6 hours under vacuum conditions. Nitrogen adsorption isotherm was determined over a relative pressure range (P/P_o) of 0.01 to 0.99. The specific surface area was measured according to Brunauer-Emmett-Teller (BET) method. The total pore volume was estimated from the amount of vapor adsorbed at relative pressure of 0.99. The micropore volume was obtained from the Dubinin-Radushkevich (DR) method. The mesopore volume was calculated by subtracting the amount of total pores with the micropores volume. The pore size distribution of the activated carbon samples was obtained by applying DFT method. Field emission scanning electron microscopy (FE-SEM) was used to observe the porous structures of the produced activated carbons.

6. Adsorption Isotherm Study

Isotherm study was conducted by fitting the data into different isotherm models, which are Langmuir, Freundlich, and Temkin. The details of each isotherm are described in Table 3. In determining the isotherm constant, it is however easier to transform the isotherm equations into linear form and then applying the linear regression as shown in Table 4.

Table 4. Isotherm model and linear regression

Isotherm	X-values	Y-values	Slope (m)	Intercept (c)
Langmuir	P	P/q_e	$1/Q_{max}$	$1/K_L \cdot Q_{max}$
Freundlich	Log P	Log q_e	1/n	Log K_F
Temkin	Ln P	q_e	RT/b	$\left(\frac{RT}{b}\right)\cdot \ln K_T$

RESULTS AND DISCUSSION

1. Analysis of Variance (ANOVA) of S/N Ratio

According to Taguchi orthogonal array, sixteen different activated carbons were prepared for methane adsorption. The methane uptake capacity of the activated carbons are listed in Table 6. ANOVA was performed to study the relative significance of the process parameters. The ANOVA for S/N ratio is shown in Table 5 with 95% confidence level. F-value indicates the statistical calculation on the effects of control factor to the response. The F-value is obtained by comparing the variance associated with the residual

Table 3. Adsorption isotherm equations and its descriptions

Isotherms	Equations	Descriptions	
Langmuir	$q_e = Q_{max}\frac{K_L P}{1+K_L P}$	q_e	: the equilibrium amount of methane gas adsorbed per kilogram of activated carbon (mol/kg)
		Q_{max}	: the complete monolayer of methane adsorption capacity
		P	: the equilibrium pressure (bar)
		K_L	: Langmuir isotherm constant
Freundlich	$q_e = K_F P^{1/n}$	q_e	: the equilibrium amount of methane gas adsorbed per kilogram of activated carbon (mol/kg)
		K_F	: Freundlich isotherm constant
		n	: the adsorption intensity
Temkin	$q_e = \frac{RT}{b}\ln(K_T P)$	K_T	: Temkin isotherm constant
		R	: Gas constant (8.314 J/mol·K)
		T	: the absolute temperature (K)
		b	: Temkin constant related to heat of sorption (J/mol)

Table 5. ANOVA for the S/N ratio

Sources	Degree of freedom	Sum of square	Mean square	F-value	P-value	Significance
Impregnation ratio	3	17.6594	5.8865	17.53	0.002	Significant
Activation temperature (°C)	3	10.351	3.4503	10.27	0.009	Significant
Activation time (min)	3	0.4378	0.1459	0.43	0.736	Insignificant
Residual error	6	2.0149	0.3358			
Total	15	30.463				

variance. It is the mean square of the factor divided with the mean square of the residual error [9]. The factor with high F-value is the most important factor affecting the methane adsorption. According to Kirby [10], an F-value of more than four indicates that the control factors have strong impact on the response. Therefore, Table 5 shows that impregnation ratio and activation temperature have strong effect on methane adsorption. On the other hand, activation time showed less effect on the preparation of AC with the lowest F-value. P-value indicates whether the control factor is significant or otherwise. The calculation of P-value is given by ANOVA Minitab software, which depends on F-value, degree of freedom of factor being tested and degree of freedom of the error [11]. A factor with P-value lower than 0.05 indicates that it is significant to response. In this case, as can be seen in Table 5, both impregnation ratio and activation temperature are significant parameters which affect the adsorption of methane with P-value lower than 0.05.

2. "Larger the Better" S/N Ratio and Optimum Condition Analysis

The term 'Signal' in this analysis stands for desired value (i.e., mean) for the response and the phrase 'Noise' denotes the undesired value (i.e., standard deviation). Thus, S/N ratio is the ratio of the mean to standard deviation [12]. Analysis of S/N ratio was used for further justification. In this study, the "larger the better" type of analysis was selected since the highest methane adsorption is always desirable. The largest S/N ratio corresponds to the optimum characteristics [13]. Table 7 summarizes the control factors and their levels on S/N ratio. As can be seen, it is clear that the optimum conditions are impregnation ratio of level 4 (0.55), activation temperature of level 4 (900 °C) and activation time of level 4 (150 min). Among these control factors, impregnation ratio is the most influential factor affecting the response. This is due to the largest difference in delta (Table 7). The adsorption capacity of an activated carbon depends largely on the presence of porous structure and surface area. $ZnCl_2$ acts as a dehydrating agent and tends to remove volatile compounds from the activated carbon and promoting bond cleavage reaction through dehydration and condensation [14]. Therefore, as can be seen in Fig. 4, increasing the impregnation ratio results in making more porous structure which contributes to high S/N ratio and high methane adsorption.

The S/N ratio for activation temperature increases as the level increases from 750 °C to 900 °C, showing that adsorption capacity was also increased. At 900 °C, the breakdown of the linkages composition of raw material was more pronounced. This could be attributed to the higher rate of activation, thus developing more pore volume [15]. The adsorption capacity of activated carbon also increased along with the prolongation of activation time. Higher activation time produces more active sites and pores on the activated carbon [7]. However, as seen in Fig. 4 the activation time had no significant gradient implying that it has very low effect on the response in comparison to the other parameters.

3. Prediction for the Optimized Value of Methane Adsorption

Based on the optimum conditions obtained from ANOVA, S/N ratio and its response, prediction of optimum value of methane adsorption can be made. Assuming that there is no interaction between the factors, the prediction of quality characteristic was cal-

Table 6. The results of confirmation test at optimum condition and comparisons with other conditions

No	Control factors			Response
	Impregnation ratio	Activation temp.	Activation time	Adsorption (mol/kg)
1	0.1	750	60	2.91
2	0.1	800	90	3.07
3	0.1	850	120	3.78
4	0.1	900	150	4.32
5	0.25	750	90	3.52
6	0.25	800	60	3.81
7	0.25	850	150	3.98
8	0.25	900	120	4.09
9	0.4	750	120	3.70
10	0.4	800	150	3.71
11	0.4	850	60	4.41
12	0.4	900	90	4.45
13	0.55	750	150	4.54
14	0.55	800	120	4.56
15	0.55	850	90	4.87
16	0.55	900	60	5.49
Optimum	0.55	900	150	6.79

Table 7. Response table for S/N ratio, larger the better

Level	Impregnation ratio	Activation temperature (°C)	Activation time (min)
1	10.82	11.18	12.14
2	11.7	11.48	11.85
3	12.15	12.55	12.08
4	**13.72**	**13.18**	**12.31**
Delta	2.90	2.00	0.46
Rank	1	2	3

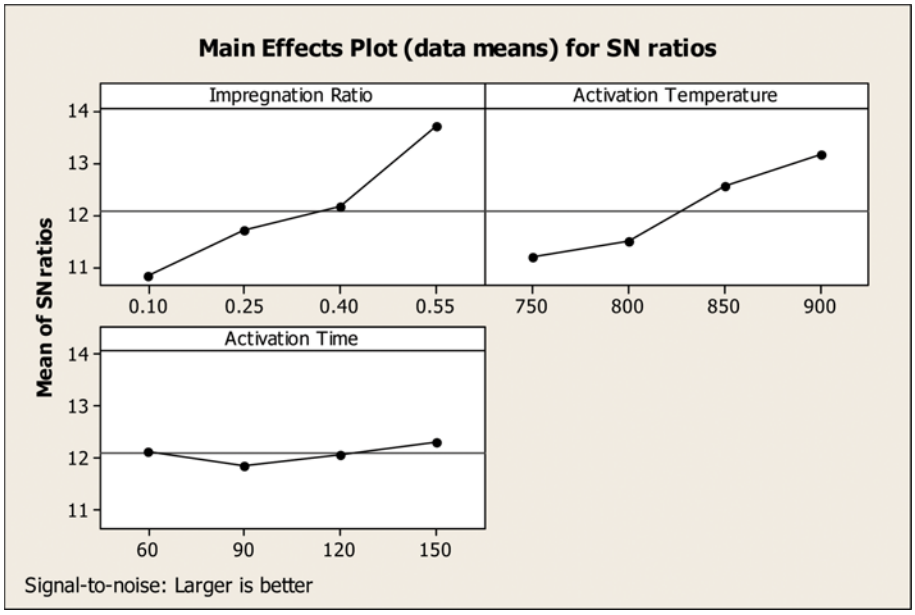

Fig. 4. The effect of control factors on S/N ratio.

culated as in Eq. (3) [16],

$$\text{Optimum predicted} = \overline{Y} + (\overline{A_4} - \overline{Y}) + (\overline{B_4} - \overline{Y}) + (\overline{C_4} - \overline{Y}) \quad (3)$$

where $\overline{Y}$ is the total average response of all experiments run, $\overline{A_4}$, $\overline{B_4}$, $\overline{C_4}$ represent chemical activation, activation temperature and activation time, respectively, with their optimal levels. The results of calculation of various response average are : $\overline{Y}$=4.07, $\overline{A_4}$=4.86, $\overline{B_4}$=4.59, $\overline{C_4}$=4.03 mol/kg. Substituting these values into Eq. (2), the predicted methane adsorption at optimum condition is 5.33 mol/kg.

The final step of confirmation experiment is to find the uncertainty of optimum value, which is also known as confidence interval (CI). If the reliability of the condition is assumed to be 95% as mentioned above, the CI can be estimated using the following equations:

$$CI = (F(\alpha, 1, f_e) \times MS_e \times ((1/N_{eff}) + (1/R)))^{0.5} \quad (4)$$

and

$$N_{eff} = N/(1 + T_{DoF}) \quad (5)$$

where $F(\alpha, 1, f_e)$ is the F-ratio required for $100(1-\alpha)$ percent confidence interval, f_e is the degree of freedom of error=6, MS_e is the mean square of residual error=0.3358, R is the number of replications of experiment=1 and N_{eff} is the effective number of replication, N is the total number of experiments=16 and T_{DoF} is the total degree of freedom associated with the optimum conditions=9 (3×3), α is the risk level (for a 95% confidence interval α is equal to 5%, hence 0.05). According to the standard F distribution table, the required F-ratio for α=0.05 is F(0.05, 1, 6)=5.9874. Thus, substituting the values in Eqs. (4) and (5), the calculated Cl equals to ±1.808. Therefore, the predicted optimum condition of methane adsorption with confidence interval of 95% is 5.33±1.808 mol/kg, i.e., the confirmation results should be in the range of 3.53 mol/kg<Optimum<7.14 mol/kg. If the result of methane adsorption in the confirmation experiment is within the range of predicted values, the overall optimization of methane adsorption by Taguchi method will be regarded as 95% reliable.

4. Confirmation Experiment of the Optimum Conditions

To validate the methane adsorption on activated carbon provided by statistical software, the activated carbon was prepared at optimum conditions. It is expected to produce the best activated carbon that would adsorb relatively high methane gas. The activated carbon prepared at optimum conditions underwent methane adsorption and the result presented in Table 6 was very satisfactory. From the table, clearly, methane adsorption on the activated carbon prepared at optimum conditions is 6.79 mol/kg which falls within the predicted 95% confidence level. The result also shows that methane uptake at optimum conditions achieved the highest amount of adsorption compared to other set of conditions.

5. Development of Regression Model

To develop a correlation between the operating parameters of activated carbon and the adsorption capacity of methane, the linear regression model was used. The regression equation was calculated by the mean values of methane adsorption under different preparation variables. The regression equation is given by:

$$\begin{aligned}\text{Methane adsorption} = &-2.18 + 2.83\ (\text{Impregnation ratio}) \\ &+ 0.00646\ (\text{Activation temperature}) \\ &+ 0.00001\ (\text{Activation time}).\end{aligned} \quad (6)$$

Based on the correlation coefficient values, the quality of the regression equation model was evaluated. The value of R^2 is the variability between the experimental data and the predicted data. In this study, the obtained R^2 is 0.8764, which explained that 87.65% of experimental data agreed well with the predicted data (shown in Fig. 5).

Fig. 6 shows the variation of errors between actual and predicted values in all experimental runs. The standard deviation of this model was 0.0443. Smaller standard deviation is good since it is showing

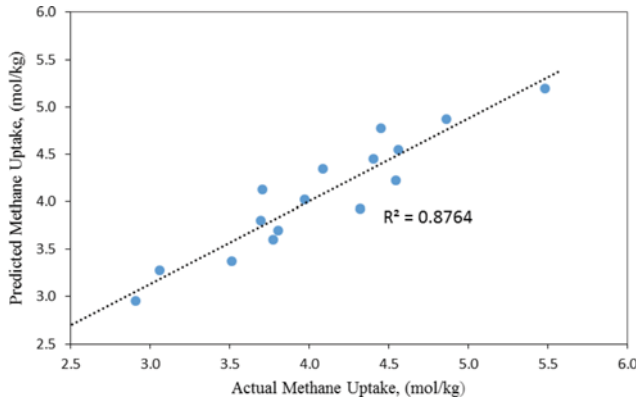

Fig. 5. Actual against predicted methane adsorption.

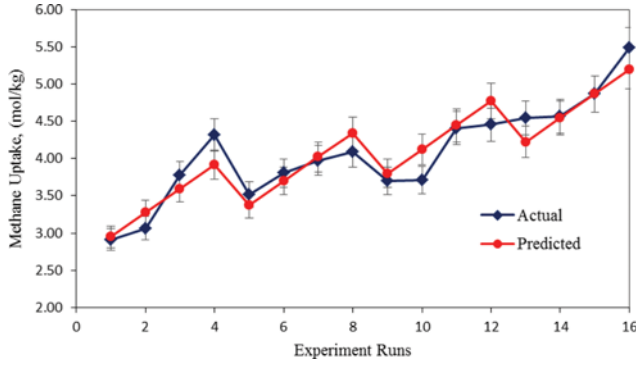

Fig. 6. Variation of errors between actual and predicted values of methane uptake.

that the model is reliable [9]. This also suggests that the predicted values were very close to the actual values.

6. Characterization of Activated Carbon Prepared at Optimum Condition

The characteristics of the activated carbons at optimum conditions were determined by N_2 adsorption/desorption, BET surface area analysis and surface morphology. Fig. 7 shows the adsorption/desorption isotherm of nitrogen at 77 K. It can be ascertained from the graph that the isotherm of activated carbon belongs to the Type IV of IUPAC classification [17], representing the adsorption isotherm with hysteresis. The Type IV shape follows the same path as Type II at low relative pressure. The sharp "knee" suggests that a considerable amount of micropores are present, and the slope of the plateau at high relative pressure is due to multilayer adsorption on non-microporous, i.e. mesoporous [18]. This indicates that the porous structures of the activated carbon are mainly microporous and mesoporous. According to Kundu et al. [6], intensive activation would increase the elimination of low molecular weight volatiles that causes development in pores. Moreover, at high temperature the micropore structure was collapsed, resulting in the formation of mesoporous activated carbon.

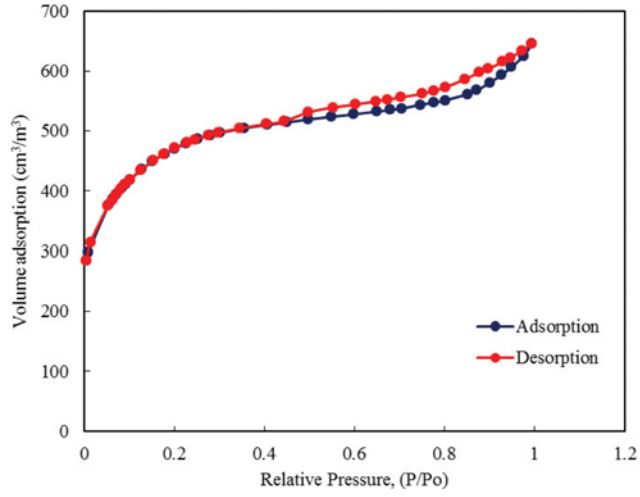

Fig. 7. N_2 adsorption on activated carbons produced at the optimum conditions.

Porous structures with high volume offer great possibility to adsorb considerable amount of methane gas in a highly dense state. From the nitrogen adsorption isotherm analysis, the BET surface area and total pore volume of the activated carbon were 1,551 m^2/g and 1.00 cm^3/g, respectively. According to Daud et al. [15], intensive rate of reaction at high temperature creates more pore volume. This might be attributed to the increase in the release of volatile matter and the removal of disorganized carbon molecules by the activation agent. Furthermore, with $ZnCl_2$ impregnation, the removal of the volatiles through the pore passage was not hindered since $ZnCl_2$ acts as a dehydrating agent during activation that inhibits tar formation and other liquid clogging [19]. Therefore, in this study, impregnation ratio of 0.55 and temperature of 900 °C with prolongation time of 150 minutes increased the release of volatile from the raw sample and therefore an increase in porous structures can be observed [20].

Fig. 8 illustrates the distribution of pore development by DFT analysis of nitrogen isotherm. The transversal dimension pores can be classified into three categories according to IUPAC classification: micropores (d<2 nm), mesopores (2 nm<d<50 nm) and macropores (d>50 nm) [21]. Based on the graph, the observed peaks are in the range of 1 to 3 nm, indicating that majority of pores are located within microporous and initial mesoporous range; thus it can be concluded that the result obtained is consistent with the N_2 isotherm trend discussed above. The proportion of micropores (58%) and mesopores (42%) of the activated carbon in this study

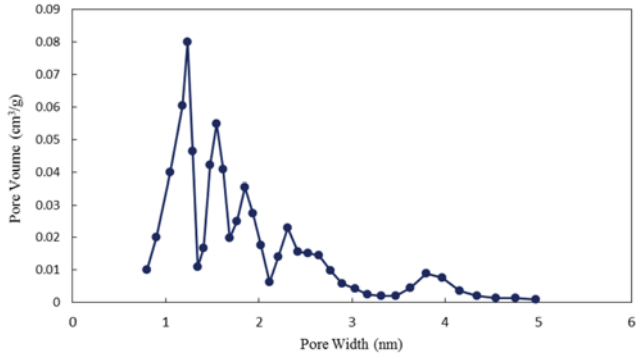

Fig. 8. DFT pore size distribution of activated carbon at optimum conditions.

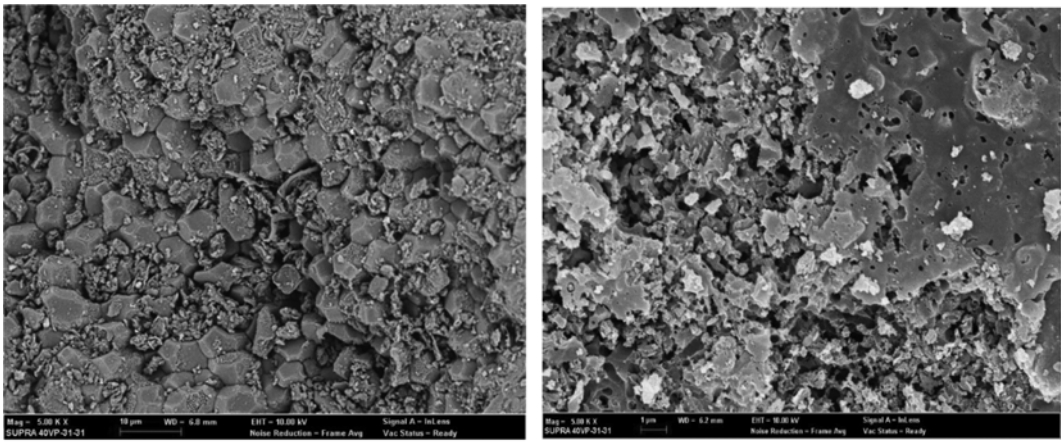

Fig. 9. Fe-SEM micropgraph of activated carbon, (a) raw precursor, (b) activated carbon at optimum conditions.

is nearly balanced. With suitable total pore size distribution, the pore wall of the activated carbon provides relatively strong attractive forces to the surrounding gas molecules. The energy of gas molecules is slowly lowered as it passes through a narrow space. As a result, gas molecules are packed densely within pore network of the carbon [22]. Since the diameter size of methane gas is about 0.4 nm [23], thus to obtain the highest gas adsorption, the pore size of activated carbon must be bigger than the size of two molecules of methane (0.8 nm) [24]. Less methane adsorption capacity is expected when activated carbon has low surface area, low volume and has very large pore size diameter. Thus, in this study, the average pore size diameter can be regarded as an appropriate size for methane gas adsorption. Too small or too large the diameter of pores is unfavourable since it may retard the adsorption process [25].

FE-SEM technique was employed to observe the surface morphology of activated carbon. The micrographs of raw PKS and PKS activated carbon are presented in Fig. 9(a) and Fig. 9(b). The raw precursors as shown in Fig. 9(a) had irregular surface structures without any significant pores except for some occasional crack. On the contrary, the image on Fig. 9(b) shows activated carbon at optimum conditions contains different size of cracks, and rougher texture on the external surface. As discussed earlier, the intensive rate of reaction at high temperature and the difference angle attack by the combination of steam and CO_2 help in creating pore networks.

The porous characteristics of various activated carbons prepared from different precursors and different conditions are compared in the Table 8. It can be observed from the data provided in the table that the BET surface area and pore volume of prepared activated carbon in this study are well enough and comparable to other literature values (Table 8).

7. Adsorption of Methane and Comparative Study

The optimum conditions and the best two activated carbons (no. 15 and no. 16) from Table 6 which obtain high methane up-

Table 8. Comparison of porous characteristics of prepared activated carbon at different operating parameter

Precursors	Chemical agent	Activation temp. (°C)	Activation time (min)	Surface area (m^2/g)	Pore volume (m^3/g)	Source
Palm Kernel Shell	$ZnCl_2$	900	120	1551	1.01	Present study
Coconut Shell	None	900	300	1653	1.08	Guo et al. [26]
Reedy Grass Leaves	$ZnCl_2$	800	120	1100	0.60	Jiangzhong et al. [27]
Coffee Endocarp	none	700	120	919	0.49	Nabais et al. [28]
Chestnut Wood	H_3PO_4	500	240	783	0.288	Gómez-Serrano et al. [29]
Olive Stone	KOH	800	120	1090	0.38	Ubago-Pérez et al. [30]
Palm Shell	$ZnCl_2$	850	420	1118	0.51	Arami-Niyya et al. [31]
Rice Straw	H_3PO_4	450	120	786	1.05	Fierro et al. [32]
Palm Shell	K_2CO_3	800	120	1170	0.48	Adinata et al. [33]
Grain Sorghum	H_3PO_4	700	15	528	0.197	Diao et al. [34]
Enteromorpha prolifera	$ZnCl_2$	700	60	1392	0.84	Li et al. [35]
Corn Corb	None	900	60	1063	0.54	Chang et al. [36]
Pistachio-Nut Shell	$ZnCl_2$	500	120	1635	0.832	Lua et al. [37]
Coconut Shell	$ZnCl_2$	900	30	1091	0.681	Azevedo et al. [38]
Hazelnut Bagasse	KOH	700	120	1489	0.932	Demiral et al. [39]

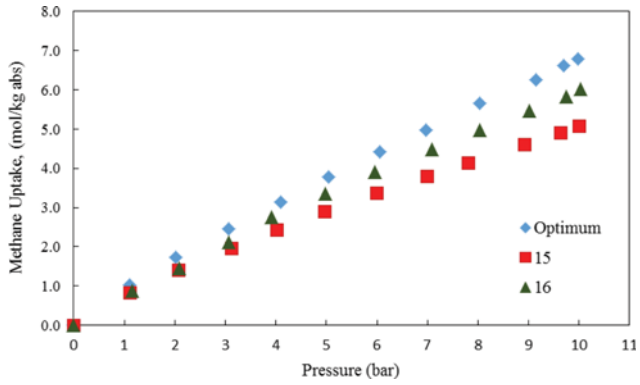

Fig. 10. Methane uptake of activated carbons prepared at different conditions.

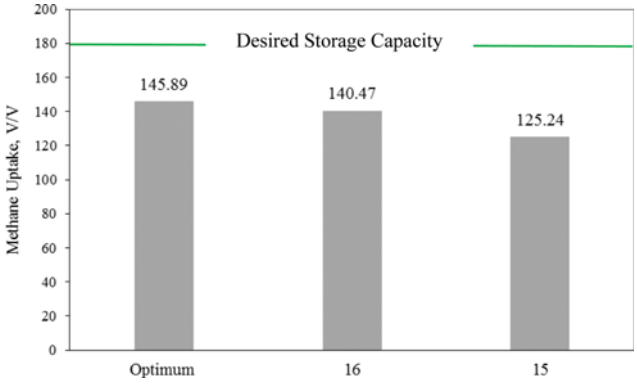

Fig. 11. Methane uptake in volumetric basis.

take underwent further analysis for methane adsorption. Fig. 10 shows the methane uptake (mol/kg) of all the three activated carbons. Methane was charged continuously until the pressure reached 15 bar and measured at 293.15 K. It can be seen clearly that methane uptake increases linearly with the pressure. The results agree well with a previous study by Arami-Niya et al. [4]. On the mass basis of methane adsorption capacity, the optimum conditions of activated carbon which were prepared under higher impregnation ratio, activation temperature and activation time recorded the highest methane uptake. High amount of methane adsorption is expected when the adsorption has large surface area and high total pore volume. In this study, it is suggested that the porosity of activated carbon prepared at optimum conditions is well developed compared to other set of conditions. As is clearly shown in Table 9, the BET surface area and total pore volume are approximately double the amount of other activated carbons. As discussed previously, the high activation reaction is due to the increase in activation temperature and time of activation while chemical impregnation facilitates the formation of larger porosity. Similar results were reported by Daud et al. [15] and Araujo et al. [38] on the porosity development.

Simultaneously, the methane uptake was analyzed in terms of volume basis. The highest methane uptake of the three activated carbons is shown in Fig. 11. The methane storage was measured at 293.15 K and 15 bars. As can be seen in the figure, the activated carbon prepared at optimum conditions recorded the highest storage capacity of 145.89 v/v. According to the Department of Energy of the United States of America, the suitable capacity of ANG storage is 180 v/v in order to be comparable with the CNG storage [38]. Thus, in general, all the activated carbons in this study showed high capacity of methane uptake on the volumetric basis. Due to the limitation of experimental equipment, however, the highest charging pressure in this study was 15 bars. Thus, it is expected that the desired storage can be achieved if further pressure is imposed on the activated carbons.

Table 10. Isotherm study of methane adsorption prepared at optimum conditions

Isotherms	Parameters	
Langmuir	Q_{max}	24.57
	K_L	0.04
	R^2	**0.9984**
Freundlich	K_F	0.88
	n	1.12
	R^2	**0.9992**
Temkin	K_T	0.97
	B (J/mol)	908.89
	R^2	**0.9352**

8. Isotherm Study

Knowledge of the adsorption equilibrium is essential to understand the interaction of molecules between gas phase (methane) and solid phase (activated carbon) at equilibrium state. The adsorption equilibrium takes place when methane surrounds the activated carbon for a certain period of time. The experimental data were fitted into linear regression isotherms and the results are shown in Table 10. The value of R^2 was used to determine the best fitted isotherm. As can be seen in Table 10, the methane adsorption on activated carbon at optimum conditions follows the Freundlich model based on the highest value of regression coefficient (R^2= 0.9992) than other model. This implies that the adsorption is non-ideal, reversible and was not restricted to the formation of monolayer (multilayer adsorption). The Freundlich isotherm shows better fit than Langmuir, suggesting the heterogeneous nature of the activated carbon. The value of n (1.17) which is greater than '1'

Table 9. Characteristics of porosity of activated carbons

Sample	SBET (m^2/g)	Vtotal (cm^3/g)	V Microporous (cm^3/g)	Microporous (%)	V Mesoporous (cm^3/g)	Mesoporous (%)
Optimum	1548.0	1.000	0.580	58.00	0.420	42.00
15	812.3	0.536	0.381	71.08	0.155	28.92
16	800.5	0.503	0.368	73.16	0.135	26.84

indicates that adsorption of methane on the activated carbon was favourable [40]. It is suggested that, at low pressure of methane adsorption, the isotherm tends to follow Freundlich model. However, when the pressure of methane adsorption reaches 50 bar and above the adsorption isotherm is favorable to fit the Langmuir equation as reported by Sreńscek-Nazzal et al. [41].

CONCLUSION

The optimization of preparation of activated carbon was successfully done using Taguchi L_{16} orthogonal arrays method and by applying the "*larger-the-better*" criterion. The optimum conditions of methane adsorption were found to be the impregnation ratio of 0.55, the activation temperature of 900 °C and the activation time of 150 min. Results of the signal to noise (S/N) ratio analysis revealed that impregnation ratio has the greatest impact among the control parameters studied. An optimized value of methane adsorption with 95% confidence level was predicted as 5.33±1.808 mol/kg. The confirmation experiment of methane adsorption at optimum condition showed methane adsorption of 6.79 mol/kg, which is within the predicted 95% confidence level. The regression model shows that 87.65% of experimental data agree well with the predicted data with small standard deviation. The characteristics of activated carbon at optimum condition suggest that activated carbon contains both microporous and mesoporous structures with nearly balanced volume percentage. The activated carbon also has intermediate structure between mesoporous and microporous with the range of pore size distribution of 1-3 nm and surface area of 1,548 m^2/g. The total pore volume was 1.0 cm^3/g having micropores and mesopores volume of 58% and 42%, respectively. The presence of opened-pore structure with different size of cracks was observed. The equilibrium data of methane adsorption on optimum activated carbon follows Freundlich isotherm based on the highest value of regression coefficient.

ACKNOWLEDGEMENTS

This study is financially supported by the Malaysian Ministry of Higher Education (MoHE) via the Fundamental Research Grant Scheme (project no: FRGS/1/2013/TK07/UiTM/02/2). Mohd Saufi Md Zaini is thankful to Universiti Teknologi MARA and MoHE for the scholarship award.

REFERENCES

1. T. Zhang, W. P. Walawender and L. T. Fan, *Bioresour. Technol.*, **101**, 1983 (2010).
2. V. C. Menon and S. Komarneni, *J. Porous Mater.*, **5**, 43 (1998).
3. A. Ahmadpour, A. Okhovat and M. J. Darabi Mahboub, *J. Phys. Chem. Solids,* **74**, 886 (2013).
4. A. Arami-Niya, W. M. A. W. Daud and F. S. Mjalli, *Chem. Eng. Res. Design*, **89**, 657 (2011).
5. S. G Herawan, M. S. Hadi, M. R. Ayob and A. Putra, *The Scientific World J.*, **2013**, 6 (2013).
6. A. Kundu, B. Sen Gupta, M. A. Hashim and G. Redzwan, *J. Cleaner Production*, **105**, 420 (2015).
7. H. Deng, G. Zhang, X. Xu, G. Tao and J. Dai, *J. Hazard. Mater.*, **182**, 217 (2010).
8. M. J. D. Mahboub, A. Ahmadpour, H. Rashidi and N. Jahanshahi, *Adsorption*, **18**, 297 (2012).
9. A. Arami-Niya, W. M. A. Wan Daud, F. S. Mjalli, F. Abnisa and M. S. Shafeeyan, *Chem. Eng. Res. Design*, **90**, 776 (2012).
10. E. D. Kirby, *The Technol. Interface Int. J.*, **7**, 1 (2006).
11. J. Casler, A. Haryanto, S. Kahle and W. Xu, *Design of experiments via Taguchi methods : one and two layouts*, Michigan Chemical Process Dynamic and Controls (2006).
12. M. Munawar, Optimization of surface finish by considering the effect of vibration in machining operations, *PhD Dissertation, Department of Industrial and Manufacturing Engineering, Univeristy of Engineering and Technology*, Lahore-Pakistan (2006).
13. P. Khare and A. Kumar, *Appl. Water Sce.*, **2**, 317 (2012).
14. M. J. Prauchner and F. Rodríguez-Reinoso, *Micropor. Mesopor. Mater.*, **152**, 163 (2012).
15. W. M. A. W. Daud, W. S. W. Ali and M. Z. Sulaiman, *J. Chem. Technol. Biotechnol.*, **78**, 1 (2003).
16. A. O. Dada, A. P. Olalaken, A. M. Olatunya and O. Dada, *J. Appl. Chem.*, **3**, 38 (2012).
17. F. Rodriguez-Reinoso, J. M. Martin-Martinez, C. Prado-Burguete and B. McEnaney, *J. Phys. Chem.*, **91**, 515 (1987).
18. J. Rouquerol, F. Rouquerol, P. Llewellyn, G. Maurin and K. S. W. Sing, *Adsorption by powders and porous solids: principles, methodology and applications*, 2nd Ed. London: Academic Press Inc. (London) Ltd. (2013).
19. J. Guo and A. C. Lua, *J. Porous Mater.*, **7**, 491 (2000).
20. R. Gottipati, Preparation and characterization of microporous activated carbon from biomass and its application in the removal of chromium (VI) from aqueous phase, *PhD Dissertation, Department of Chemical Engineering, National Institute of Technology Rourkela*, Odisha (2012).
21. W. M. A. W. Daud and W. S. W. Ali, *Bioresour. Technol.*, **93**, 63 (2004).
22. I. Prasetyo, R. Yunanto and T. Ariyanto, Methane Storage by Methane Hydrate Formation within Water-saturated Porous Carbon : The Effect of Mesoporosity, *In: Chemeca 2011: Engineering a Better World*, Engineers Australia, 599 (2011).
23. K. Mosher, *The Impact of Pore Size on Methane and CO_2 Adsorption in Carbon*, MSc Dissertation, Department of Energy Resources Engineering, Stanford University (2011).
24. C. Almansa, M. Molina-Sabio and F. Rodríguez-Reinoso, *Micropor. Mesopor. Mater.*, **76**, 185 (2004).
25. J. Liu, Y. Zhou, Y. Sun, W. Su and L. Zhou, *Carbon*, **49**, 3731 (2011).
26. S. Guo, J. Peng, W. Li, K. Yang, L. Zhang, S. Zhang and H. Xia, *Appl. Surface Sci.*, **255**, 8443 (2009).
27. X. Jianzhong, C. Lingzhi and F. Xiaojie, Preparation and characterization of activated carbon from reedy grass Leaves in a two-step activation procedure, *In the Proceedings of International Conference on Material and Environmental Engineering* (2014).
28. J. M. V. Nabais, P. Nunes, P. J. M. Carrott, M. M. L. Ribeiro Carrott, A. M. García and M. A. Díaz-Díez, *Fuel Process. Technol.*, **89**, 262 (2008).
29. V. Gómez-Serrano, E. M. Cuerda-Correa, M. C. Fernández-González, M. F. Alexandre-Franco and A. Macías-García, *Mater. Lett.*, **59**,

846 (2005).
30. R. Ubago-Pérez, F. Carrasco-Marín, D. Fairén-Jiménez and C. Moreno-Castilla, *Micropor. Mesopor. Mater.*, **92**, 64 (2006).
31. A. Arami-Niya, W. M. A. W. Daud and F. S. Mjalli, *J. Anal. Appl. Pyroly.*, **89**, 197 (2010).
32. V. Fierro, G. Muñiz, A. Basta, H. El-Saied and A. Celzard, *J. Hazard. Mater.*, **181**, 27 (2010).
33. D. Adinata, W. M. A. W. Daud and M. K. Aroua, *Bioresour. Technol.*, **98**, 145 (2007).
34. Y. Diao, W. Walawender and L. T. Fan, *Bioresour. Technol.*, **81**, 45 (2002).
35. Y. Li, Q. Du, X. Wang, P. Zhang, D. Wang, Z. Wang and Y. Xia, *J. Hazard. Mater.*, **183**, 583 (2010).
36. C.-F. Chang, C.-Y. Chang and W.-T. Tsai, *J. Colloid Interface Sci.*, **232**, 45 (2000).
37. A. C. Lua and T. Yang, *J. Colloid Interface Sci.*, **290**, 505 (2005).
38. D. C. S. Azevedo, J. C. S. Araújo, M. Bastos-Neto, A. E. B. Torres, E. F. Jaguaribe and C. L. Cavalcante, *Micropor. Mesopor. Mater.*, **100**, 361 (2007).
39. H. Demiral, I. Demiral, F. Tümsek and B. Karabacakoğlu, *Surface Interface Anal.*, **40**, 616 (2008).
40. H. Zheng, D. Liu, Y. Zheng, S. Liang and Z. Liu, *J. Hazard. Mater.*, **167**, 141 (2009).
41. J. Sreńscek-Nazzal, W. Kamińska, B. Michalkiewicz and Z. C. Koren, *Industrial Crops and Products*, **47**, 153 (2013).